Structure, Magnetic Properties and Magnetic Phase Diagram of a Layered, Bimetallic, Cyanide-Bridged Cr^{III}-Ni^{II} Metamagnet

Arnaud Marvilliers,[a] Simon Parsons,[b] Eric Rivière,[a] Jean-Paul Audière,[a] Mohamedally Kurmoo,[c] and Talal Mallah*[a]

To the memory of Olivier Kahn to whom we owe a great deal

Keywords: Chromium / Cyanides / Magnetic properties / Nickel

The reaction of hexacyanochromate(III) with $Ni(tmc)^{2+}$ (tmc = tetramethylcyclam) leads to the formation of the layered compound $[Ni(tmc)]_3[Cr(CN)_6]_2{\cdot}18H_2O$ displaying a corrugated sheet structure. Within each layer, the Ni(tmc) units are surrounded by two $Cr(CN)_6$ complexes in a *trans* fashion while the $Cr(CN)_6$ units are linked to three Ni(tmc) molecules in facial positions. The magnetic studies show ferromagnetic interaction for a $Ni^{II}(d^8, t_{2g}^6e_g^2)$–CN–$Cr^{III}(d^3, t_{2g}^3)$ system within the layers. Below a critical temperature (T_N = 14 K), a bulk antiferromagnetic order is observed due to a small interlayer antiferromagnetic interaction. An antiferromagnetic → ferromagnetic phase transition occurs for an applied field H_C of 1200 Oe expressing the metamagnetic behavior of the compound. The phase diagram of the compound was constructed and the antiferromagnetic interlayer magnetic energy was estimated to be equal to 0.1 cm^{-1}.

Introduction

Over the last ten years, bimetallic, cyanide-bridged systems built from hexacyanometallates have provided new materials possessing three,[1−9] two,[10−16] one[17−21] and zero[22−27] dimensionality.[28] Room temperature molecular-based magnets as well as photoinduced magnets have been synthesized and characterized.[4,29−32] Kahn and coworkers opened new perspectives in the field by preparing a $Mo^{III}-Mn^{II}$ cyanide-bridged, three-dimensional ferromagnet (T_C = 51 K) possessing large magnetic anisotropy.[33,34]

The magnetic properties are intimately related to the dimensionality of the systems. When the cyanide bridges spread in the three directions of space, long-range magnetic ordering occurs. On the other hand, if the cyanide bridges are restricted in zero dimensions, leading to high-spin discrete species,[22,23,26,27] new phenomena like the blocking and the quantum tunneling of the magnetization may be observed.[35,36]

We report here the preparation, crystal structure, magnetic properties and magnetic phase diagram of a new compound $[Cr(CN)_6]_2[Ni(tmc)]_3{\cdot}18H_2O$ obtained from the reaction of $[Ni(tmc)](ClO_4)_2$ (tmc = tetramethylcyclam, a tetradentate ligand) and $K_3[Cr(CN)_6]{\cdot}2H_2O$.

[a] Laboratoire de Chimie Inorganique, UMR 8613, Université Paris-Sud,
91405 Orsay, France
Fax: (internat.) +33-1/6915-4754
E-mail: mallah@icmo.u-psud.fr
[b] Department of Chemistry, The University of Edinburgh, West Mains Road, Edinburgh, EH9 3JJ, United Kingdom
[c] Institut de Physique et Chimie des Matériaux de Strasbourg, UMR 7504,
23, rue du Loess, 67037 Strasbourg, France

Supporting information for this article is available on the WWW under http://www.wiley-vch.de/home/eurjic or from the author.

Results and Discussion

Synthesis and Characterization

The reaction of $[Ni(tmc)](ClO_4)_2$ and $K_3[Cr(CN)_6]{\cdot}2H_2O$ in water leads to the formation of an insoluble pale pink powder. The IR spectrum of the powder shows the presence of all the features expected for the organic tmc ligand in addition to two bands at 2154 and 2129 cm^{-1} assigned to the asymmetric vibrations of bridging and nonbridging cyanides. Elemental analysis is consistent with the following formula $[Cr(CN)_6]_2[Ni(tmc)]_3{\cdot}18H_2O$. In order to estimate accurately the number of water molecules and to study the effect of dehydration, thermogravimetry was carried out in

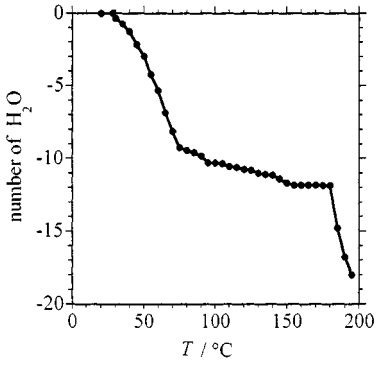

Figure 1. Thermogravimetric analysis in the form of loss of water molecules per unit formula versus temperature

  1434−1948/01/0505−1287 $ 17.50+.50/0

the temperature range 20−190 °C. Upon heating, nine water molecules are lost between room temperature and 75°C (Figure 1).

A further three water molecules are lost between 75 and 185 °C, where decomposition occurs. A total loss of 12 water molecules per unit formula is thus observed, although chemical analysis gave a total of 18 water molecules per unit formula. The remaining six water molecules are possibly more strongly bound through hydrogen bonds. The IR spectrum of a powder heated up to 180 °C and that of a nonheated sample are identical. The IR spectrum of the powder heated above 185 °C shows the absence of many bands belonging to the organic ligand.

Single crystals were obtained by a slow diffusion of aqueous solutions of the two precursors in an H tube. The IR spectrum of a few crystals was found to be identical to that of the powder.

Structure

X-ray diffraction studies reveal a layered structure with corrugated sheets as depicted in Figure 2 and 3. Within each layer, each Ni(tmc) unit is surrounded by two hexacyanochromate complexes in a *trans* position, as expected, while the $Cr(CN)_6$ units are linked to three Ni(tmc) disposed in a facial manner. The observed honeycomb-like corrugated layers are the result of: (i) the facial and not the meridional disposition of the three nickel complexes around the chromium anion, and (ii) the presence of an inversion center located on the nickel atoms. The same spatial arrangement has already been found in a related compound reported earlier where the tetradentate ligand cyclam were used instead of tetramethylcyclam.[12]

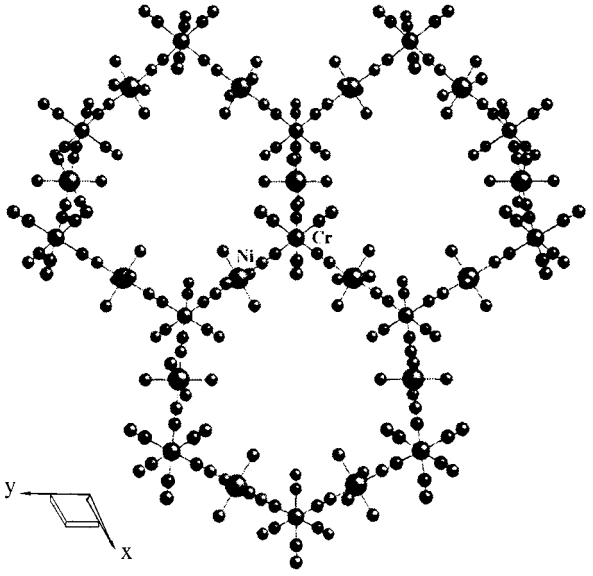

Figure 2. View along the *z* axis showing the honeycomb-like structure of the layers

All chromium atoms are crystallographically equivalent within the structure. The geometry around Cr can be considered as being isotropic. Around the nickel, the shortest distance [Ni(1)−N(10) = 2.089(10)Å] is that with the cyanides′ nitrogen atoms. The Ni−N bonds to the tmc′s nitrogen atoms are 2.185(18) and 2.306(14) Å for Ni(1)−N(1) and Ni(1)−N(4) respectively (Figure 4).

Despite the high *R* factor (14%), there is a clear tendency to have longer Ni−N bonds within the macrocycle than with the apical cyanides′ nitrogen atoms. This lengthening has already been noted for cyclam derivatives.[37] It has been attributed to the nonbonded repulsion between the hydrogen atoms of the alkyl substituents and those of adjacent carbon atoms. This bond lengthening within the macrocycle results in a shortening of the apical Ni−N bond lengths when axial ligands are present. Indeed, the apical Ni−N bond lengths are shorter for *trans*-[Ni(tetrapropylcyclam)$(NCS)_2$] than for *trans*-[Ni(cylam)(NCS).[38,39] The same tendency is observed when comparing the data of the present compound to those of the previously reported cyclam analogue. The shortest Ni−N bond length is found for nitrogen atoms belonging to the organic macrocycle [Ni−N = 2.06(2) Å] for the cyclam analogue, while for the present compound the apical Ni−N bond length is found to be the shortest. Another important difference between the two compounds is the value of the Ni(1)−N(10)−C(10) angle [173.4(1)°] which is closer to linearity in the present compound than when cyclam is used [171.6(1)°].

Magnetic Properties

All the magnetic studies were performed on a powdered sample and it was checked that the properties of a few single crystals were the same as that of the powder. The $\chi_M T = f(T)$ curve (Figure 5, recorded in an applied field of 3000 Oe) shows that $\chi_M T$ increases smoothly between 300 and 50 K upon cooling and then sharply below 50 K. A maximum is observed at $T = 14$ K. The $\chi_M T$ value at $T = 300$ K (8.18 cm^3 K mol^{-1}) is well above what is expected for two noninteracting Cr^{III} and three noninteracting Ni^{II} ions i.e. 7.03 cm^3 K mol^{-1}, obtained by fitting the high temperature part of the $1/\chi_M = f(T)$ curve.[40]

The increase of $\chi_M T$ upon cooling is the signature of a ferromagnetic-exchange coupling between nearest neighbor metal ions through the cyanide bridge. This has already been observed in related systems and has been ascribed to the orthogonality of the Cr^{III} and Ni^{II} magnetic orbitals.[2,22,26] The abrupt increase of $\chi_M T$ below 50 K to a maximum value as large as 156 cm^3 K mol^{-1} indicates the occurrence of a large correlation between the magnetic ions within the layers which is the origin of the magnetic anisotropy within the compound.[41]

In order to investigate the low temperature behavior, the temperature dependence of the magnetization was first measured in the presence of a weak applied field (30 Oe) and then at higher fields ranging from 400 to 1400 Oe.[42] The susceptibility (*M*/*H*) vs. temperature curve performed at $H = 30$ Oe (Figure 6) reveals the presence of a maximum at $T = 14$ K. The presence of such a maximum rules out the possibility of a 3D ferromagnetic order, where a saturation of the susceptibility is expected.

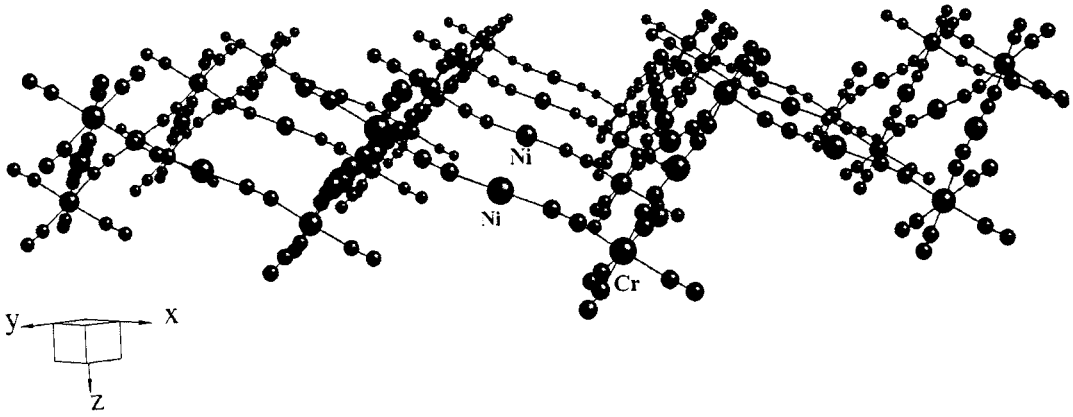

Figure 3. View along the *xy* plane revealing the corrugated sheets (tmc has been removed for clarity)

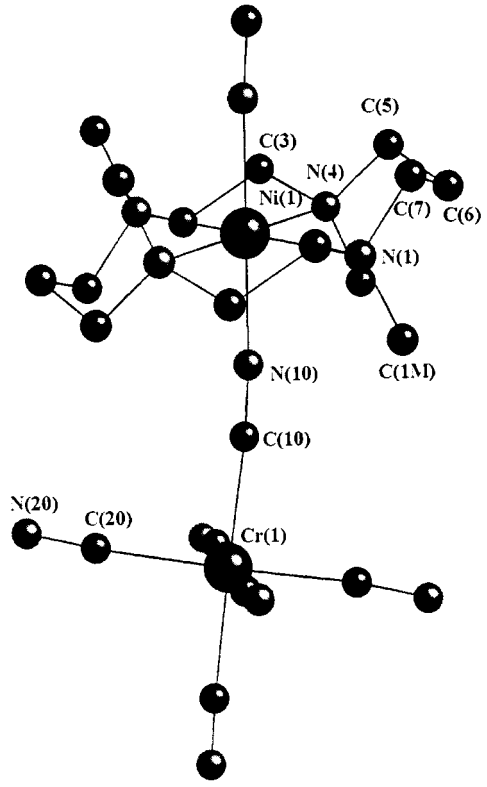

Figure 4. View of a dinuclear unit with atom-numbering scheme (hydrogen atoms are omitted for clarity); selected bond lengths [Å] and angles [°] with standard variations in parentheses: Ni(1)−N(1) 2.185(18), Ni(1)−N(4) 2.306(14), Ni(1)−N(10) 2.089(10), C(10)−N(10) 1.141(14), C(20)−N(20) 1.075(13), Cr(1)−C(10) 2.067(9), Cr(1)−C(20) 2.103(9); C(10)−N(10)−Ni(1) 173.4(10), N(10)−C(10)−Cr(1) 173.6(10), N(10)−C(20)−Cr(1) 174.7(11)

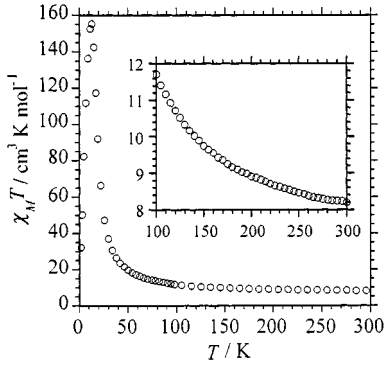

Figure 5. Thermal variation of the product of susceptibility and temperature of $[Cr(CN)_6]_2[Ni(tmc)]_3 \cdot 18H_2O$ ($\chi_M T$ versus T) in an applied field H = 3 kOe; inset: the increase of $\chi_M T$ between 300 and 100 K

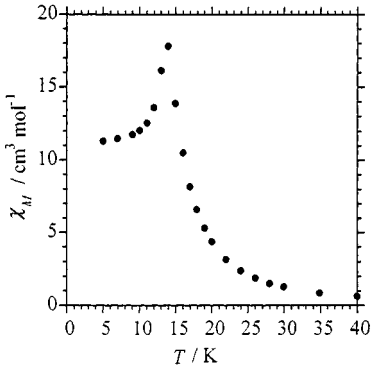

Figure 6. Thermal variation of the susceptibility in a field of 30 Oe

On the other hand, the fact that at low temperature (5 K) the susceptibility value (11.3 cm^3 mol^{-1}) is about two thirds that at the maximum (17.8 cm^3 mol^{-1}) is the signature of the occurrence of antiferromagnetic ordering in a randomly nonoriented sample.[43] For antiferromagnets in noncubic symmetry and within the framework of the mean field approximation, the perpendicular and the parallel components of the susceptibility measured on a single crystal have the same value at the ordering temperature. Below T_N, the perpendicular component remains constant in order to minimize the magnetic energy while the value of the parallel component decreases and vanishes at low temperature. Since the susceptibility of a powder is given by $\chi = (\chi_{\parallel} + 2\chi_{\perp})/3$, its value expected at low temperature corresponds to two thirds that of the maximum, as observed experimentally in the present compound.

Upon increasing the strength of the applied magnetic field, the maximum of the $M = f(H)$ curves (Figure 7) shifts

towards low temperature and disappears beyond $H = 1400$ Oe, showing a saturation of the magnetization.

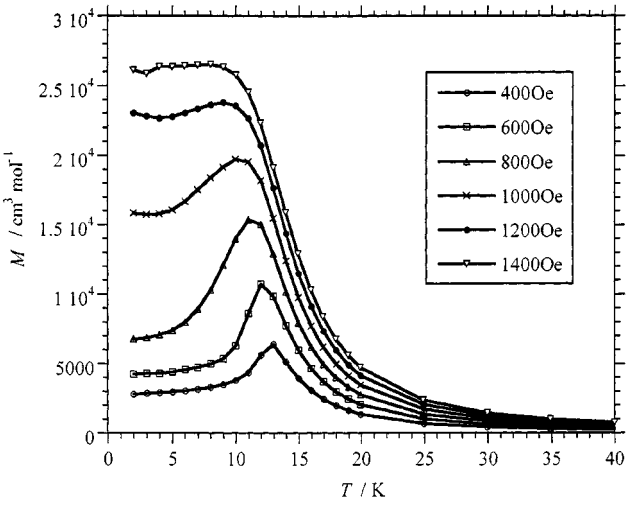

Figure 7. Thermal variation of the magnetization of a polycrystalline sample for different applied magnetic fields

This is the signature of the appearance of a ferromagnetic phase induced by the external applied magnetic field. On the other hand, the magnetization vs. field measurements performed at $T = 2$ K (Figure 8) present a sigmoidal shape. Upon increasing the applied field from zero, the magnetization increases first linearly and then abruptly and reaches saturation around 7 kOe. The sigmoidal shape of the $M = f(H)$ curve is characteristic of a metamagnetic behavior. This is the result of the transition from an antiferromagnetic to a field-induced ferromagnetic phase without going through an intermediate spin-flop phase. Such an abrupt transition is observed only if magnetic anisotropy is of the same order of magnitude or larger than the antiferromagnetic interaction so that the antiparallel magnetic moments remain in the same direction as the increasing applied magnetic field. In the case where the anisotropy energy is weaker than the antiferromagnetic energy, beyond a given magnetic field (which is usually very small) the system goes through an intermediate phase with canted magnetic moments (the spin-flop phase) before reaching the ferromagnetic phase. In such a situation, upon increasing the applied magnetic field a linear increase of the magnetization that extrapolates to zero for $H = 0$ should be observed before saturation is reached.[44,45] Such metamagnetic behavior has been already observed in layered compounds with strong ferromagnetic intralayer interactions and relatively weak interlayer antiferromagnetic interactions so that the magnetic anisotropy energy need not be very strong. The critical field needed to overcome the antiparallel alignment of the magnetic moments is found to be equal to 1170 Oe at $T = 2$K.

In summary, we can conclude that within the layers a ferromagnetic interaction operates leading to a relatively large correlation between the magnetic ions, while between the layers a weak antiferromagnetic interaction occurs leading to an overall antiferromagnetic order at $T_N = 14$ K. This antiferromagnetic order is overcome by an external applied field of 1170 Oe at $T = 2$ K.

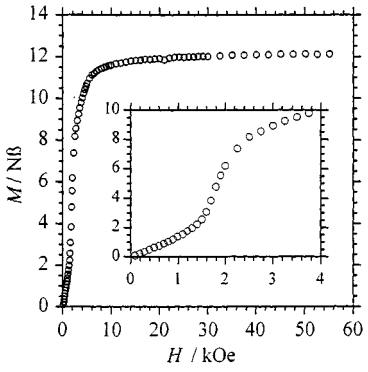

Figure 8. Variation of the magnetization as a function of the applied magnetic field at $T = 2$ K; inset: the sigmoidal shape at low values of the field

Magnetization vs. field isotherms performed at temperatures ranging from 2 to 14 K (not shown here) demonstrate that the critical field value decreases upon increasing the temperature and vanishes at $T = 14$ K. The critical field is estimated at the intersection of two linear slopes before and after the transition. Plotting the critical field H_C(T) as a function of the temperature at which the magnetization isotherms are measured leads to the phase diagram of the metamagnet (Figure 9). This phase diagram (which is partial as explained below) presents two regions delimited by the H_C(T) = f(T) curve. The region below the curve corresponds to the domain of stability of the antiferromagnetic phase while the upper region corresponds to the domains where the field-induced ferromagetic and the paramagnetic phases are stable. These two phases are, of course, well separated but a frontier line is difficult to determine experimentally.

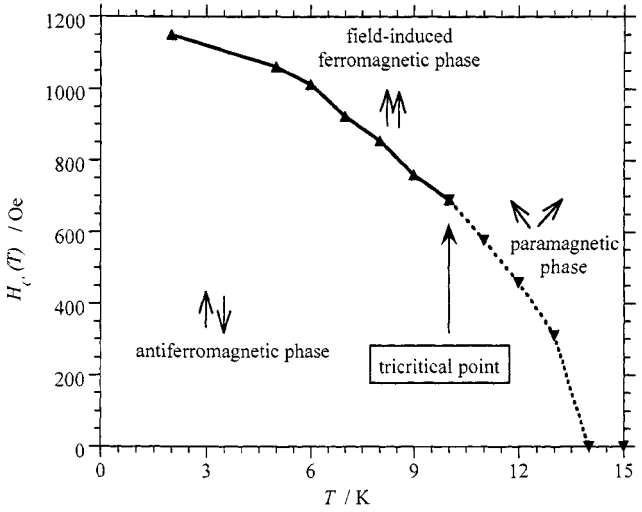

Figure 9. Phase diagram of the metamagnet; the dashed curve represents the range of second order magnetization and the continuous curve represents first order hysteresis magnetization; the tricritical point separates the two regions

However, a metamagnet has a tricritical point (T_{TCP} in the following discussion) where the three phases coexist; this tricritical point belongs to the H_C(T) = f(T) curve.[45] At temperatures below T_{TCP} the antiferromagnetic−ferromagnetic transition is a first order trans-

ition and a hysteresis loop should be observed in the $M = f(H)$ curves, while at temperatures above that of the tricritical point (but below T_N), the antiferromagnetic−paramagnetic phase transition is a second order transition and no hysteresis loop can be present. So, in order to determine the temperature of the tricritical point, we measured the magnetization as a function of the applied field for temperatures ranging from 2 to 12 K. Figure 10 shows the presence of a hysteresis loop in the $M = f(H)$ curve performed at $T = 2$ K.

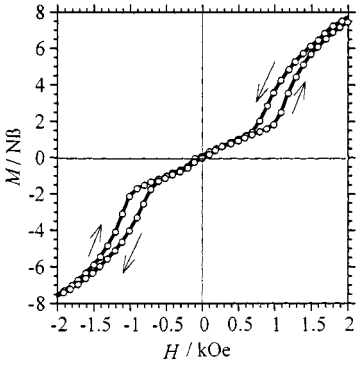

Figure 10. Hysteresis curve recorded between −2 and +2 kOe at $T = 2$ K

The maximum width of the loop is found to be equal to 244 Oe. When the temperature is increased, the width of the hysteresis loop decreases to 70 Oe at $T = 9$ K and almost vanishes at 10 K (Figure 11). Between 10 and 13 K, the $M = f(H)$ curves still have the sigmoidal shape (less pronounced than at lower temperatures) but no hysteresis could be detected anymore. This allows us to place the tricritical point at $T_{TCP} = 10$ K.

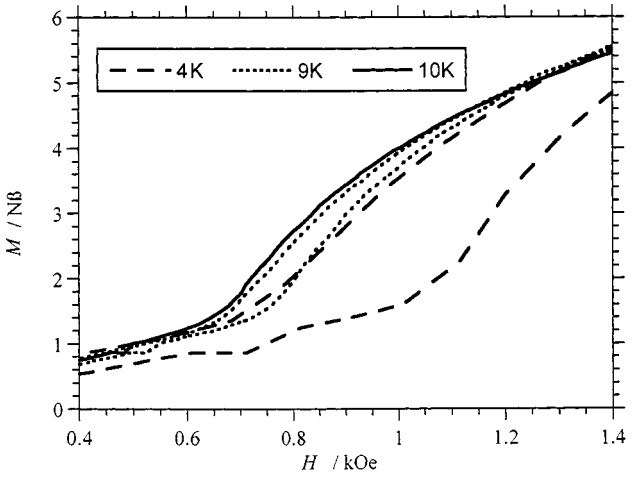

Figure 11. Isothermal magnetization curves measured at $T = 4$ K (-----), 9 K (·····) and 10 K (—); note the hysteresis behavior at 9 and 4 K

The value of the critical field H_C of the metamagnet may be obtained by extrapolating the $H_C(T) = f(T)$ curve to $T = 0$ K; it is found to be equal to 1200 Oe. This corresponds to the magnetic field needed to overcome the antiparallel alignment of the spins. The corresponding magnetic energy is given by $g\beta H_C$ and is found to be equal to 0.1 cm^{-1} when assuming a g value of 2.

Concluding Remarks

The quality of the crystal structure of this compound is not high enough to allow a thorough discussion of the origin of the bulk magnetic properties reported. For instance, the position of the water molecules that occupy the interlayer space (18 per unit formula) could not be refined and there was no possibility of knowing whether a hydrogen-bonded network exists within the compound. However, TGA studies show that six water molecules (per unit formula) cannot be removed before decomposition (which occurs at a rather high temperature). This suggests that these water molecules belong to a hydrogen-bonded network spreading all over the compound and linking the layers together. On the other hand, the magnetic properties of a sample heated at 180 °C under vacuum for 24 hours are the same as those of a nonheated sample. This is in line with the hypothesis of the presence of water molecules linking the layers through hydrogen bonds and thus forming a pathway for the interlayer antiferromagnetic interaction responsible for the antiferromagnetic order. The magnitude of the magnetic energy corresponding to the interlayer antiferromagnetic interaction (0.1 cm^{-1}) is weak but reasonable for a separation of 9.25 Å between the layers. This is still in a distance range where exchange through bonds may be more important than through space (dipolar).

The metamagnetic behavior observed is the result of the presence of a magnetic anisotropy with an energy at least as large as the energy responsible for the antiferromagnetic interaction between the layers. A quantitative determination of the magnetic anisotropy energy may be obtained from single crystal magnetic studies. Unfortunately, such studies could not be carried out because of a lack of crystals of suitable size and shape. However, the large correlation between the magnetic moment evidenced by the rather large value of the susceptibility at the Néel temperature is responsible for the presence of the magnetic anisotropy that leads to the metamagnetic behavior. The large correlation is the result of a relatively large ferromagnetic exchange interaction through the cyanide bridge. The lack of such a correlation in the previously reported cyclam analogue indicates that the magnitude of the $Cr^{III}-Ni^{II}$ ferromagnetic interaction is larger in the present tmc-based compound.[12,46] This may be related to the local structure around the Ni atoms; shorter apical Ni−N bond lengths and Ni−N−C angles (NC being the cyanide bridges) closer to linearity in the present compound may be the origin of the larger ferromagnetic short-range interaction and thus responsible for the bulk magnetic properties observed in the present compound and absent in the cyclam analogue.

Experimental Section

Hazards: Perchlorate salts should be handled with care and used in small quantities.

Syntheses: The $[Ni(tmc)](ClO_4)_2$ salt was prepared as previously reported.[47] The powder samples of the reported compound were obtained as follows: an aqueous solution (50 mL) containing 10^{-3} mol of $[Ni(tmc)](ClO_4)_2$ was added dropwise to 50 mL of an aqueous solution containing an equimolar amount of $K_3[Cr(CN)_6]\cdot 2H_2O$. A pale pink powder immediately formed, which was filtered, thoroughly washed with water and then dried under vacuum. – $C_{54}H_{132}Cr_2N_{24}Ni_3O_{18}$ (1685.9): calcd. C 37.67, H 7.67, N 19.53, Ni 10.24, Cr 6.05; found C 37.61, H 7.70, N 19.49, Ni 10.13, Cr 5.93.

General Remarks: Thermogravimetric studies were carried out in argon atmosphere at a heating rate of 1 °C per minute. The magnetic measurements were performed using a SQUID magnetometer operating in the 300–2 K temperature range and the 0–55 kOe magnetic field range. The drawings were carried out with the CRYSTAL MAKER program.[48]

Crystal Data for 1: $C_{54}H_{132}Cr_2N_{24}Ni_3O_{18}$, M = 1685.97, trigonal, a = 16.055(4), c = 9.248(7) Å, U = 2064.4(17) Å^3, T = 220 K, space group $P\bar{3}m1$, Z = 1, Cu-$K_{\alpha 1}$ = 3.461 mm^{-1}, 3503 reflections measured, of which 1161 were unique (R_{int} = 0.0745). The structure was solved by direct methods (SIR92) and refined with Shelxl-97;[49,50] solvent water was treated in the manner described by van der Sluis and Spek.[51] The final conventional R factor [based on F and 788 data with $F > 4(F)$] was 0.1465. The high R factor reflects complete disorder of the macrocycle about the crystallographic 2/m site occupied by the Ni. Crystallographic data (excluding structure factors) for the structures reported in this paper have been deposited with the Cambridge Crystallographic Data Centre as supplementary publication no. CCDC 147292. Copies of the data can be obtained free of charge on application to CCDC, 12 Union Road, Cambridge CB2 1EZ UK [Fax: (internat.) +44-1223/336-033; E-mail: deposit@ccdc.cam.ac.uk).

Acknowledgments

The authors thank Dr. Jean-Pierre Renard for interesting discussions and the CNRS (Centre National de Recherche Scientifique) for financial support.

[1] D. Babel, *Comments Inorg. Chem.* **1986**, *5*, 285.
[2] V. Gadet, T. Mallah, I. Castro, M. Verdaguer, P. Veillet, *J. Am. Chem. Soc.* **1992**, *114*, 9213–9124.
[3] T. Mallah, S. Thiébaut, M. Verdaguer, P. Veillet, *Science* **1993**, *262*, 1554–1557.
[4] S. Ferlay, T. Mallah, R. Ouahès, M. Verdaguer, P. Veillet, *Nature* **1995**, *378*, 701–703.
[5] W. R. Entley, G. S. Girolami, *Science* **1995**, *268*, 397–400.
[6] M. S. El Fallah, E. Rentshler, A. Caneschi, R. Sessoli, D. Gatteschi, *Angew. Chem. Int. Ed. Engl.* **1996**, *35*, 1947–1949.
[7] W. E. Bushmann, S. C. Paulson, C. M. Wynn, M. A. Girtu, A. J. Epstein, H. S. White, J. S. Miller, *Adv. Mater.* **1997**, *9*, 645–646.
[8] S. Ferlay, T. Mallah, R. Ouahès, P. Veillet, M. Verdaguer, *Inorg. Chem.* **1999**, *38*, 229–234.
[9] M. Ohba, N. Usaki, N. Fukita, H. Okawa, *Angew. Chem. Int. Ed.* **1999**, *38*, 1795–1797.
[10] M. Ohba, H. Okawa, T. Ito, A. Ohto, *J. Chem. Soc., Chem. Commun.* **1995**, 1545–1946.
[11] N. Re, E. Gallo, C. Floriani, H. Miyasaka, N. Matsumoto, *Inorg. Chem.* **1996**, *35*, 6004–6008.
[12] S. Ferlay, T. Mallah, J. Vaissermann, F. Bartolomé, P. Veillet, M. Verdaguer, *Chem. Commun.* **1996**, 2481–2482.
[13] M. Ohba, H. Okawa, N. Fukita, Y. Hashimoto, *J. Am. Chem. Soc.* **1997**, *119*, 1011–1019.
[14] H. Miyasaka, N. Matsumoto, N. Re, E. Gallo, C. Floriani, *Inorg. Chem.* **1997**, *36*, 670–676.
[15] N. Re, R. Crescenzi, C. Floriani, H. Miyasaka, N. Matsumoto, *Inorg. Chem.* **1998**, *37*, 2717–2722.
[16] E. Colacio, J. M. Dominguez-Vera, M. Ghazi, R. Kivekés, F. Lloret, J. M. Moreno and H. Stoeckli-Evans, *Chem. Commun.* **1999**, 987–988.
[17] G. O. Morpugo, V. Mosini, P. Porta, G. Dessy, V. Fares, *J. Chem. Soc., Dalton Trans.* **1981**, 111–117.
[18] M. Ohba, N. Maruono, H. Okawa, T. Enoki, J.-M. Latour, *J. Am. Chem. Soc.* **1994**, *116*, 11566–11577.
[19] M. Ohba, N. Fukita, H. Okawa, *J. Chem. Soc., Dalton Trans.* **1997**, 1733–1737.
[20] M. Ohba, N. Usuki, N. Fukita, H. Okawa, *Inorg. Chem.* **1998**, *37*, 3349–3354.
[21] A. Marvilliers, S. Parsons, E. Rivière, J. -P. Audière, T. Mallah, *Chem. Commun.* **1999**, 2217–2218.
[22] T. Mallah, C. Auberger, M. Verdaguer, P. Veillet, *J. Chem. Soc., Chem. Commun.* **1995**, 61–62.
[23] A. Scuiller, T. Mallah, A. Nivorozkhin, M. Verdaguer, P. Veillet, *New J. Chem.* **1996**, 1–3.
[24] K. Van Langenberg, S. R. Batten, K. J. Berry, D. C. R. Hockless, B. Moubaraki, K. S. Murray, *Inorg. Chem.* **1997**, *36*, 5006–5015.
[25] A. Marvilliers, T. Mallah, E. Rivière, S. Parsons, C. Muñoz, K. E. Vostrikova, *Mol. Cryst. Liq. Cryst.* **1999**, *335*, 1195–1206.
[26] A. Marvilliers, Y. Pei, J. Cano Boquera, K. E. Vostrikova, C. Paulsen, E. Rivière, J.-P. Audière, T. Mallah, *Chem. Commun.* **1999**, 1951–1952.
[27] G. Rogez, A. Marvilliers, E. Rivière, J.-P. Audière, F. Lloret, F. Varret, A. Goujon, N. Mendenez, J.-J. Girerd, T. Mallah, *Angew. Chem. Int. Ed.* **2000**, *39*, 2885–2887.
[28] Here we restrict the word dimensionality to coordination bonds, a two dimensional system is one where coordination bonds (metal–cyanides, for example) spread in the two directions of space.
[29] S. M. Holmes, G. S. Girolami, *J. Am. Chem. Soc.* **1999**, *121*, 5593–5594.
[30] E. Dujardin, S. Ferlay, X. Phan, C. Desplanches, C. Cartier dit Moulin, P. Sainctavit, F. Baudelet, E. Dartyge, P. Veillet, M. Verdaguer, *J. Am. Chem. Soc.* **1998**, *120*, 11347–11352.
[31] O. Sato, T. Iyoda, A. Fujishima, K. Hashimoto, *Science* **1996**, *272*, 704–705.
[32] O. Sato, Y. Einaga, A. Fujishima, K. Hashimoto, *Inorg. Chem.* **1999**, *38*, 4405–4412.
[33] J. Larionova, R. Clérac, J. Sanchiz, O. Kahn, S. Golhen, L. Ouahab, *J. Am. Chem. Soc.* **1998**, *120*, 13088–13095.
[34] J. Larionova, O. Kahn, S. Golhen, L. Ouahab, R. Clérac, *J. Am. Chem. Soc.* **1999**, *121*, 3349–3356.
[35] T. Mallah, S. Ferlay, A. Scuiller, M. Verdaguer, NATO ASI Series C vol. 484, *Magnetism: A Supramolecular Function* **1996**, p.597–614.
[36] N. Vernier, G. Bellessa, T. Mallah, M. Verdaguer, *Phys. Rev. B* **1997**, *56*, 75–76.
[37] A. E. Martell, R. D. Hancock, R. J. Motekaitis, *Coord Chem. Rev.* **1994**, *133*, 39–92.
[38] N. W. Alcock, A. C. Benniston, S. J. Grant, H. A. A. Omar, P. Moore, *J. Chem. Soc., Chem. Commun.* **1991**, 1573–1574.
[39] T. Ito, M. Kato, H. Ito, *Bull. Chem. Soc. Jpn.* **1984**, *57*, 2641–2643.
[40] The $\chi_M T$ value of 7.03 for noninteracting metal ions allows us to compute the g value for Ni^{II} which is found to be equal to 2.10 assuming a g value of 1.99 for Cr^{III}.
[41] The value of $\chi_M T$ has no real meaning because at this temperature the magnetization is field dependent, nevertheless the high value indicates the presence of a large correlation within the layers.
[42] It was checked that ac susceptibility vs. temperature plots performed at 0 and 50 Oe static applied field are identical to those of Figure 6 which indicate that saturation effects are nonexistent at such low fields. On the other hand, such measurements made at different frequencies of the oscillating field and with zero static field confirm the presence of a magnetic ordering at T = 14 K.
[43] A. Herpin, in *Théorie du magnétisme* **1968**, pp. 472–498.
[44] We must be cautious at this stage because our measurements

were carried out on a powder and not on an oriented single crystal with the applied field parallel to the easy axis, but the shape of the $M = f(H)$ curve, which is the sum of the parallel and the perpendicular components of the magnetization, presents a too sharp transition to be that of a spin-flop phase.

[45] L. J. de Jongh, A. R. Miedema, *Adv. Phys.* **1974**, *23*, 1−260.

[46] For the previously reported cyclam-based compound, the largest susceptibility value measured (within the same applied field as for the present compound i.e. 30 Oe) was found to be one order of magnitude smaller than for the present compound.

[47] E. K. Barefield, F. Wagner, *Inorg. Chem.* **1973**, *12*, 2435−2439.

[48] D. Palmer, *CrystalMaker*, Bicester, **1993**.

[49] A. Altomare, G. Cascarano, C. Giacovazzo, A. Guagliardi, *J. Appl. Crystallogr.* **1993**, *26*, 343−350.

[50] G. M. Sheldrick, Institüt für Anorganische Chemie der Universität, Tammanstraße 4, 3400 Göttingen, Germany, **1998**.

[51] H. v. d. Sluis, A. L. Spek, *Acta Crystallogr., Sect A* **1990**, *46*, 194−201.

Received September 7, 2000
[I00337]